
This copy is for your personal, non-commercial use only.

If you wish to distribute this article to others, you can order high-quality copies for your colleagues, clients, or customers by [clicking here](#).

Permission to republish or repurpose articles or portions of articles can be obtained by following the guidelines [here](#).

The following resources related to this article are available online at www.sciencemag.org (this information is current as of July 12, 2011):

Updated information and services, including high-resolution figures, can be found in the online version of this article at:

<http://www.sciencemag.org/content/333/6039/218.full.html>

Supporting Online Material can be found at:

<http://www.sciencemag.org/content/suppl/2011/07/07/333.6039.218.DC1.html>

This article **cites 21 articles**, 10 of which can be accessed free:

<http://www.sciencemag.org/content/333/6039/218.full.html#ref-list-1>

This article appears in the following **subject collections**:

Development

<http://www.sciencemag.org/cgi/collection/development>

ancestors (Fig. 2, B and C) ($i > l$: $F_{1,104} = 27.9$; $P < 0.0001$; $o > r$: $F_{1,60} = 166.2$; $P < 0.0001$), thus indicating reciprocal coevolution in the outcrossing host populations. Whereas the obligate selfing populations in the coevolution treatment became more infected over time (Fig. 2A), the wild-type populations maintained the same level of infectivity over the course of the experiment (Fig. 2B) ($g = l$: $F_{1,104} = 0.35$; $P = 0.554$), while the obligate outcrossing populations were significantly less infected at the end of the experiment relative to the beginning (Fig. 2C) ($m > r$: $F_{1,60} = 33.1$; $P < 0.0001$). Coupled with the maintenance of high outcrossing rates in the coevolving wild-type populations (Fig. 1), these results demonstrate the ability of antagonistic coevolution to continually generate novel environmental conditions under which outcrossing is favored and populations persist when interacting with a virulent pathogen.

A recent host/pathogen coevolution study in *C. elegans* further supports the conclusion that low levels of outcrossing impede the rate of adaptive evolution. The *C. elegans* hosts in this previous study appear to have primarily reproduced via self-fertilization and did not evolve significantly greater resistance to a coevolving pathogen over 48 generations of selection (27). Contrary to our study, however, greater outcrossing rates did not evolve in these mixed-mating populations in response to the pathogen. It may be that higher levels of genetic variation and/or a greater level of pathogen virulence in our study account for the difference in outcomes.

In summary, we found that obligately selfing lineages were driven to extinction when con-

fronted with a coevolving parasite. These results are consistent with the macroevolutionary aspects of the Red Queen hypothesis, as originally formulated by Van Valen (28). We also found that the presence of a coevolving pathogen selected for and maintained high levels of outcrossing in mixed-mating populations, whereas elevated levels of outcrossing were not maintained in populations where the pathogen was not coevolving. These results are consistent with the microevolutionary predictions of the Red Queen. Taken together, the results demonstrate that sex can facilitate adaptation to novel environments, but the long-term maintenance of sex requires that the novelty does not wear off.

References and Notes

- G. C. Williams, *Sex and Evolution* (Princeton University Press, Princeton, NJ, 1975).
- J. Maynard Smith, *The Evolution of Sex* (Cambridge University Press, Cambridge, UK, 1978).
- G. Bell, *The Masterpiece of Nature: The Evolution and Genetics of Sexuality* (University of California Press, Berkeley, CA, 1982).
- G. L. Stebbins, *Am. Nat.* **91**, 337 (1957).
- L. T. Morran, M. D. Parmenter, P. C. Phillips, *Nature* **462**, 350 (2009).
- H. J. Muller, *Am. Nat.* **66**, 118 (1932).
- R. A. Fisher, *The Genetical Theory of Natural Selection* (Clarendon Press, Oxford, 1930).
- R. Lande, D. W. Schemske, *Evolution* **39**, 24 (1985).
- D. Charlesworth, B. Charlesworth, *Annu. Rev. Ecol. Syst.* **18**, 237 (1987).
- A. F. Agrawal, C. M. Lively, *Evolution* **55**, 869 (2001).
- J. Jaenike, *Evol. Theory* **3**, 191 (1978).
- W. D. Hamilton, *Oikos* **35**, 282 (1980).
- W. D. Hamilton, R. Axelrod, R. Tanese, *Proc. Natl. Acad. Sci. U.S.A.* **87**, 3566 (1990).
- C. M. Lively, *Nature* **328**, 519 (1987).

- K. C. King, L. F. Delph, J. Jokela, C. M. Lively, *Curr. Biol.* **19**, 1438 (2009).
- C. M. Lively, C. Craddock, R. C. Vrijenhoek, *Nature* **344**, 864 (1990).
- E. Decaestecker *et al.*, *Nature* **450**, 870 (2007).
- B. Koskella, C. M. Lively, *Evolution* **63**, 2213 (2009).
- J. Jokela, M. F. Dybdahl, C. M. Lively, *Am. Nat.* **174** (suppl. 1), S43 (2009).
- S. Paterson *et al.*, *Nature* **464**, 275 (2010).
- S. Brenner, *Genetics* **77**, 71 (1974).
- H. Teotónio, D. Manoel, P. C. Phillips, *Evolution* **60**, 1300 (2006).
- L. M. Miller, J. D. Plenefisch, L. P. Casson, B. J. Meyer, *Cell* **55**, 167 (1988).
- T. Schedl, J. Kimble, *Genetics* **119**, 43 (1988).
- C. L. Kurz *et al.*, *EMBO J.* **22**, 1451 (2003).
- G. V. Mallo *et al.*, *Curr. Biol.* **12**, 1209 (2002).
- R. D. Schulte, C. Makus, B. Hasert, N. K. Michiels, H. Schulenburg, *Proc. Natl. Acad. Sci. U.S.A.* **107**, 7359 (2010).
- L. Van Valen, *Evol. Theory* **1**, 1 (1973).

Acknowledgments: We thank H. Hundley and R. Matteson for logistical assistance. We also thank F. Bashey, L. Delph, P. Phillips, M. Parmenter, the Lively and Hall laboratories, and two reviewers for helpful comments and discussion, as well as the Wissenschaftskolleg zu Berlin for a fellowship to C.M.L. during the preparation of the manuscript. Funding was provided by the NSF (DEB-0640639 to C.M.L.) and the NIH (1F32GM096482-01 to L.T.M.). Nematode strains were provided by the *Caenorhabditis* Genetics Center, which is funded by the NIH National Center for Research Resources (NCRR). Data deposited at Dryad, 10.5061/dryad.c0q0h.

Supporting Online Material

www.sciencemag.org/cgi/content/full/333/6039/216/DC1
Materials and Methods

Fig. S1

Table S1

References 29 to 31

31 March 2011; accepted 24 May 2011

10.1126/science.1206360

Isolation of Single Human Hematopoietic Stem Cells Capable of Long-Term Multilineage Engraftment

Faiyaz Notta,^{1,2*} Sergei Doulatov,^{1,2*} Elisa Laurenti,^{1,2} Armando Poepl,¹ Igor Jurisica,^{3,4} John E. Dick^{1,2†}

Lifelong blood cell production is dependent on rare hematopoietic stem cells (HSCs) to perpetually replenish mature cells via a series of lineage-restricted intermediates. Investigating the molecular state of HSCs is contingent on the ability to purify HSCs away from transiently engrafting cells. We demonstrated that human HSCs remain infrequent, using current purification strategies based on Thy1 (CD90) expression. By tracking the expression of several adhesion molecules in HSC-enriched subsets, we revealed CD49f as a specific HSC marker. Single CD49f⁺ cells were highly efficient in generating long-term multilineage grafts, and the loss of CD49f expression identified transiently engrafting multipotent progenitors (MPPs). The demarcation of human HSCs and MPPs will enable the investigation of the molecular determinants of HSCs, with a goal of developing stem cell-based therapeutics.

Mature blood cell lineages are generated from a network of hierarchically distinct progenitors that arise from self-renewing hematopoietic stem cells (HSCs). The extensive regenerative potential of HSCs makes them attractive targets for cellular and genetic

therapies. The molecular regulation of specific HSC properties such as long-term self-renewal is beginning to be elucidated for murine HSCs (1). However the biology of human HSCs remains poorly understood because of their rarity and the lack of methods to segregate HSCs from multipotent progenitors (MPPs) to obtain pure populations for biological and molecular analysis.

otient progenitors (MPPs) to obtain pure populations for biological and molecular analysis.

The bulk of HSCs are CD34⁺, as evidenced by human transplantation and xenograft repopulation assays; however, most CD34⁺ cells are lineage-restricted progenitors and HSCs remain rare. HSCs can be enriched further on the basis of CD45RA (2), Thy1 (3–5), and CD38 (6, 7) expression. Loss of Thy1 expression in the CD34⁺CD38[−]CD45RA[−] compartment of lineage-depleted cord blood (CB) was recently proposed to be sufficient to separate HSCs from MPPs (5). However, more than a third of Thy1[−] primary recipients gave rise to engraftment in secondary animals, raising uncertainty about whether Thy1 can absolutely segregate HSCs from MPPs. To

¹Division of Stem Cell and Developmental Biology, Campbell Family Institute for Cancer Research/Ontario Cancer Institute, Toronto, Ontario, Canada. ²Department of Molecular Genetics, University of Toronto, Toronto, Ontario, Canada. ³Ontario Cancer Institute and Campbell Family Institute for Cancer Research, Toronto, Ontario, Canada. ⁴Departments of Computer Science and Medical Biophysics, University of Toronto, Toronto, Ontario, Canada.

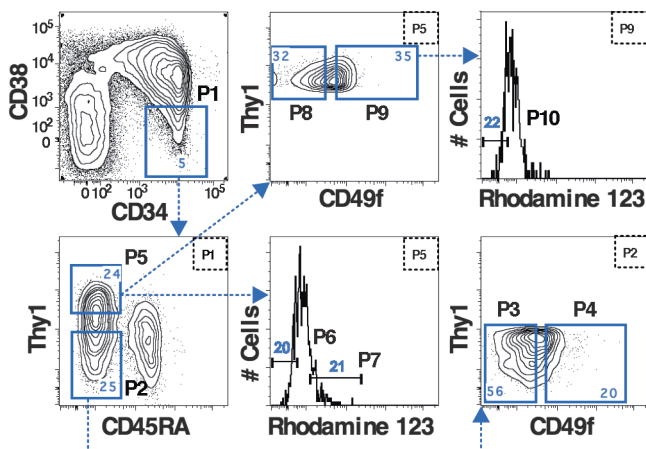
*These authors contributed equally to this work.

†To whom correspondence should be addressed. Toronto Medical Discovery Tower, Room 8-301, 101 College Street, Toronto, Canada M5G 1L7. E-mail: jdick@uhnres.utoronto.ca

resolve the relationship between these two subsets, the number of cells in each subset that are capable of short-term and long-term engraftment must be quantified at clonal resolution. We recently optimized the HSC xenograft assay by using intrafemoral injection into female NOD-*scid*-

IL2Rgc^{-/-} (NSG) mice (8–10). Flow-sorted CB HSCs (CD34⁺CD38⁻CD45RA⁻Thy1⁺; Thy1⁺) (Fig. 1, P5) and MPPs (CD34⁺CD38⁻CD45RA⁻Thy1⁻; Thy1⁻) (Fig. 1, P2) fractions were functionally characterized with our HSC assay. A priori, HSCs were operationally defined by lymphomyeloid

Fig. 1. Cell sorting scheme used to isolate human HSCs and MPPs. Lin⁻ CB cells were stained with monoclonal antibodies against CD34, CD38, CD45RA, Thy1 (CD90), CD49f antigens, and the mitochondrial membrane dye Rho. The frequency of each subpopulation (P1 to P10) is based on the parent gate shown on the top right of each plot.



engraftment that persisted for at least 20 weeks after transplant. This duration represents a stringent test of long-term repopulation and encompasses the total engraftment time of primary and secondary transplants historically used to assess the self-renewal capacity of human HSCs in xenograft models. At nonlimiting cell doses, recipients of Thy1⁺ and Thy1⁻ cells had similar levels of human chimerism and lineage distribution (injected femur: $P = 0.17$; Fig. 2, A and B; fig. S1; and table S1). To assess whether Thy1⁻ cells would persist beyond the allotted 20-week primary transplant period, we performed secondary transplants for an additional 12 to 14 weeks. This revealed that Thy1⁻ cells could be serially transplanted, albeit with lower efficiency than Thy1⁺ cells (table S2), which is consistent with previous work (5). These data suggest that cells with extensive self-renewal potential exist in both Thy1⁺ and Thy1⁻ subsets, although the basis for the disparity in secondary transfer efficiency between these subsets remained unknown.

We next performed limiting dilution analysis (LDA) to measure the frequency of HSCs within Thy1⁺ and Thy1⁻ fractions. One in 20 Thy1⁺ cells (5%) clonally initiated long-term hematopoiesis in NSG mice as compared to 1 in 100 (1%) Thy1⁻ cells ($P = 0.0003$, Fig. 2C). Double sorting and high-stringency sort modes used in our experimental design ruled out the possibility that HSC activity from Thy1^{lo/+} cells (figs. S2 and S3). The inability of prior studies to detect engraftment from Thy1⁻ cells was probably due to the less sensitive xenograft models employed (3). Thus, although Thy1⁺ enriches for HSCs, long-term repopulating activity persists in the Thy1⁻ fraction previously believed to represent MPPs (5).

To examine the hierarchical relationship between the Thy1 subsets, we cultured sorted Thy1⁺ and Thy1⁻ cells with stroma cells known to express HSC-supportive ligands (11). Both Thy1⁺ and Thy1⁻ cells (>70%) remained CD34⁺CD38⁻ on stromal cultures (fig. S4, column 3). Unexpectedly, Thy1⁻ cells consistently generated Thy1⁺ cells on stroma (Fig. 2D, right panel) and also in vivo within the bone marrow microenvironment of NSG mice that received transplants (Fig. 2E). Thy1⁺ cells arising from Thy1⁻ cells after culture, as well as Thy1⁺ cells that retained their Thy1 expression, had robust repopulating activity in NSG mice 20 weeks after transplantation. Engraftment and lineage potentials were identical for Thy1⁺ cells derived from either Thy1 subfraction (Fig. 2F and fig. S5). Cells that remained Thy1⁻ after being cultured on OP9 stroma did not sustain a long-term graft (Fig. 2F, right panel); however, they transiently repopulated (fig. S6). These results demonstrate that the Thy1⁻ compartment is heterogeneous and contains a small fraction with repopulating activity and a larger fraction with MPP-like activity.

To further purify HSCs in both Thy1⁺ and Thy1⁻ subsets, we searched for a different cell

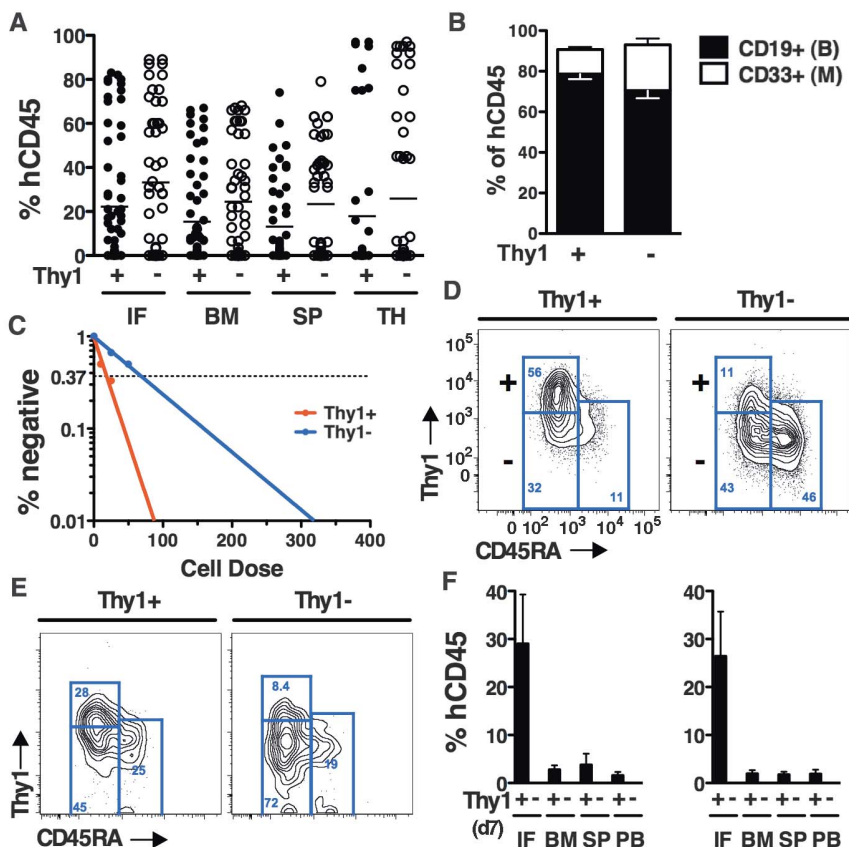


Fig. 2. Functional characterization of the Thy1⁺ and Thy1⁻ subsets. (A and B) Engraftment and lineage potential of Thy1⁺ (P5) and Thy1⁻ (P2) cells assessed in NSG mice 20 weeks after transplant (Thy1⁺: $n = 65$ mice; Thy1⁻: $n = 30$ mice, 6 experiments). IF, injected femur; BM, left femur, tibiae; SP, spleen; TH, thymus. (C) Frequency of long-term repopulating cells within Thy1⁺ and Thy1⁻ populations measured by LDA. (D) Phenotype of Thy1⁺ (left) and Thy1⁻ (right) cells cultured on OP9 stroma. Plots are gated on CD34⁺CD38⁻ cells (figs. S4 and S14). (E) Phenotype of Thy1⁺ and Thy1⁻ cells engrafted in NSG mice. (F) Populations labeled + and - from (D) were isolated from stroma and transplanted into NSG mice (200 to 400 cells, two experiments, $n = 10$ mice per group). Their engraftment potential (as percent of CD45⁺ cells) is shown in the bottom panel. All data are presented as means \pm SEM. PB, peripheral blood.

surface marker. We hypothesized that integrins would mark human HSCs, because they mediate niche interactions and have been used to isolate murine HSCs and other somatic stem cells (12, 13). We compared the surface expression of several adhesion molecules between HSC-enriched (Thy1⁺) and -depleted (Thy1⁻) fractions. Among our candidates, only ITGA6 (integrin $\alpha 6$, termed CD49f) was differentially expressed (Fig. 3A and fig. S7), with 50 to 70% of Thy1⁺ cells expressing CD49f versus 10 to 20% of Thy1⁻ cells.

To determine whether human HSCs could be delineated using CD49f expression, we partitioned Thy1⁺ cells into CD49f^{+/hi} (here called Thy1⁺CD49f⁺; Fig. 1, P9) and CD49f^{lo/-} (here called Thy1⁺CD49f⁻; Fig. 1, P8) subfractions and evaluated their capacity for long-term multilineage chimerism in NSG recipients. Mean chimerism in the injected femur was 6.7-fold higher for Thy1⁺CD49f⁺ than for Thy1⁺CD49f⁻ cells (22.7% versus 3.4%, $P < 0.0001$, Fig. 3B, left panel), and only Thy1⁺CD49f⁺ cells could be serially transplanted (table S3). LDA revealed that 9.5% (1 in 10.5) of Thy1⁺CD49f⁺ cells had long-term repopulating activity as compared with 0.9% (1 in 111.3) Thy1⁺CD49f⁻ cells ($P = 9.9 \times 10^{-9}$, Fig. 3C, and tables S1 and S4). Because we had found that the Thy1⁻ fraction was heterogeneous, we tested whether CD49f expression also marked Thy1⁻ HSCs. Indeed, only Thy1⁻CD49f⁺ cells reconstituted NSG mice 20 weeks after transplant (Fig. 3B, right panel). LDA indicated that approximately 4.5% (1 in 22.1) of cells in this fraction had long-term multilineage engraftment potential as compared to 0.13% (1 in 735.2) of Thy1⁻CD49f⁻ cells (Fig. 3C and table S4). No difference in lineage potential was observed between Thy1⁺CD49f⁺ and Thy1⁻CD49f⁺ cells (fig. S8), although recipients of Thy1⁺CD49f⁺ cells trended toward higher levels of chimerism at similar cell doses (table S1). We estimate that although most human HSCs are Thy1⁺, consistent with prior work, 1 in 5.5 CB HSCs lack Thy1 expression. These data indicate that human HSCs are marked by CD49f, and they establish the existence of Thy1⁻ HSCs.

The absence of long-term grafts in Thy1⁻CD49f⁻ recipients raised the possibility that the loss of CD49f demarcated human MPPs in the Thy1⁻ subset (5). To test this idea, we temporally monitored the peripheral blood and marrow of NSG recipients transplanted with all four Thy1 and CD49f subsets for 30 weeks. Although levels of chimerism gradually increased in the peripheral blood of mice transplanted with CD49f⁺ HSC subsets, engraftment of Thy1⁻CD49f⁻ cells peaked between 2 and 4 weeks and then declined (Fig. 3D). The bone marrow of Thy1⁻CD49f⁻ recipients displayed significantly higher levels of chimerism at 2 weeks than did CD49f⁺ HSCs in both the injected femur and noninjected bones, indicating that Thy1⁻CD49f⁻ cells have a higher engraftment and differentiation potential than HSCs immediately after transplant (Fig. 3E). These

results also rule out the idea that Thy1⁻CD49f⁻ cells have impaired capacity to home and proliferate in the marrow. B cells, monocytes, granulocytes, and erythrocytes were detected in the bone marrow of Thy1⁻CD49f⁻ mice (Fig. 3E and fig. S9). HSC-enriched fractions displayed a delay in engraftment until 4 weeks (Fig. 3F). The engraftment kinetics of Thy1⁺CD49f⁻ cells were intermediate to HSC and Thy1⁻CD49f⁻ subsets (Fig. 3, D to F). These data demonstrate that Thy1⁻CD49f⁻ cells can give rise to all major hematopoietic lineages but fail to engraft long-term, indicating that these are bona fide MPPs. To remain consistent with previous work (5), we

defined transiently engrafting Thy1⁻CD49f⁻ cells as MPPs. However, considering that Thy1⁻CD49f⁻ cells differ from CD49f⁺ HSCs solely in the ability to engraft durably, an alternate interpretation is that Thy1⁻CD49f⁻ cells are short-term HSCs.

To provide an independent line of evidence for distinguishing our functionally defined HSC and MPP populations, we carried out global gene expression analysis of sorted CD49f⁺ and Thy1⁻CD49f⁻ subsets. Unsupervised hierarchical clustering revealed that the CD49f⁺ HSCs clustered together irrespective of Thy1 status (fig. S10A). No significant differences in gene expression were detected between these subsets,

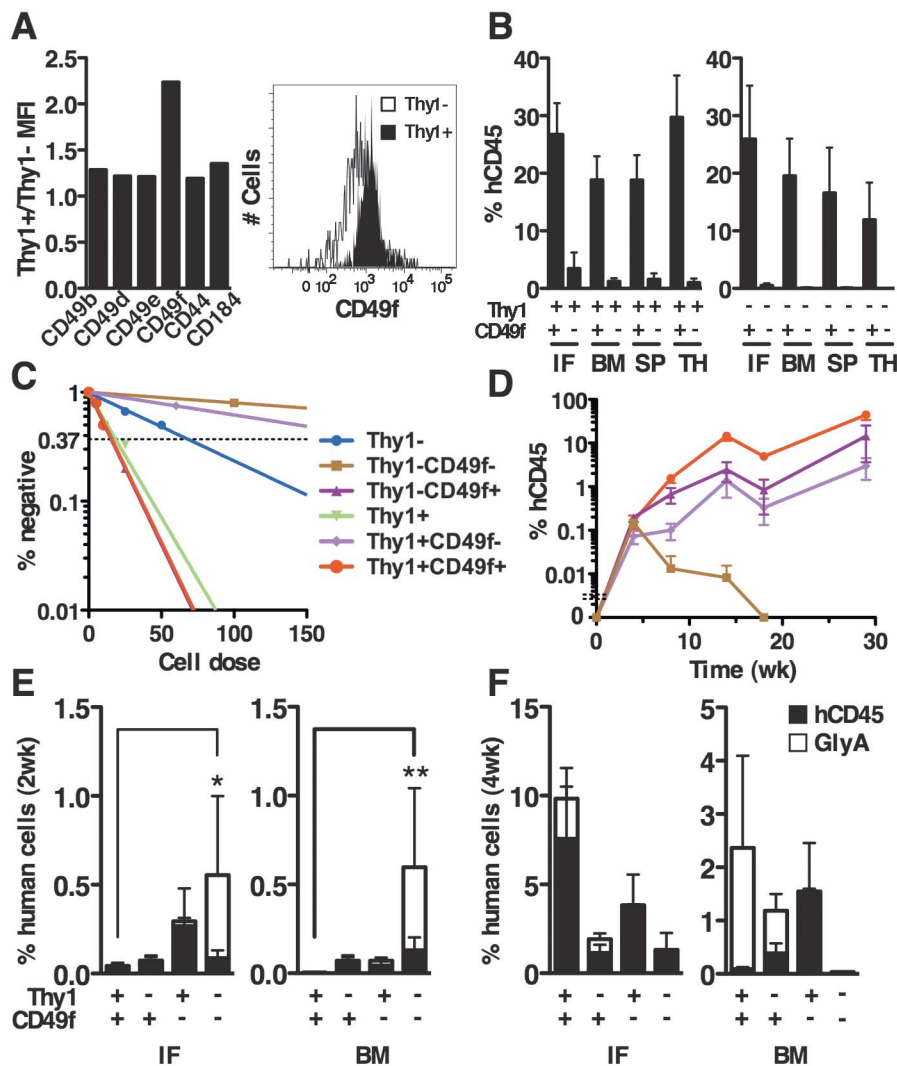


Fig. 3. Human HSCs and MPPs are demarcated by CD49f expression. (A) Cell surface expression of adhesion molecules (CD49b, CD49d, CD49e, CD49f, CD44, and CD184) measured as the ratio of mean fluorescence intensity (MFI) between HSC-enriched (Thy1⁺) and -depleted (Thy1⁻) populations. (B) Mean engraftment levels of cells fractionated by Thy1 and CD49f expression in NSG mice ($n = 4$ experiments). Cell doses and number of mice are shown in table S1. (C) Long-term repopulating cell frequency in Thy1 and CD49f subsets measured by LDA. (D) Kinetic analysis of peripheral blood engraftment (measured as percent of CD45⁺ cells) by cells fractionated on Thy1 and CD49f after transplantation into NSG mice (100 to 200 cells per recipient). The legend is consistent with (C). (E and F) Short-term engraftment by cells fractionated on Thy1 and CD49f at 2 (E) and 4 (F) weeks after transplant. The human graft consisted of GlyA⁺ erythroid (white bars) and CD45⁺ myelolymphoid cells (black bars). All data are presented as means \pm SEM. * $P < 0.05$; ** $P < 0.001$. BM, non-injected bones.

although $\text{Thy1}^- \text{CD49f}^+$ HSCs displayed an intermediate pattern to $\text{Thy1}^+ \text{CD49f}^+$ HSCs and MPPs (fig. S10B), consistent with the lower frequency of HSCs within this population. In contrast, the $\text{Thy1}^- \text{CD49f}^-$ MPPs clustered independently from both CD49f^+ HSC subsets (fig. S10A). Seventy differentially expressed genes segregated $\text{Thy1}^- \text{CD49f}^-$ MPP versus HSC subsets (fig. S10B and table S5), consistent with previous murine studies (14). Stem and committed progenitor cells (15) differed more dramatically (500 to 3000 genes), underscoring the close relationship between immature cell types. These findings support our functional delineation of $\text{Thy1}^+ \text{CD49f}^+$ and $\text{Thy1}^- \text{CD49f}^+$ HSCs as distinct from $\text{Thy1}^- \text{CD49f}^-$ MPPs and identify gene expression changes associated with the earliest steps of human HSC differentiation.

Although sorting based on CD49f enables the highest reported purity of human HSCs, this test still falls short of the most definitive assessment of HSC potential: single-cell transplantation. A single long-term mouse HSC provides lifelong blood production (16). Because only 9.5% of $\text{Thy1}^+ \text{CD49f}^+$ cells were HSCs by LDA, additional strategies were needed to efficiently assess single human HSCs. High efflux of the mitochondrial dye rhodamine-123 (Rho) could enrich for HSCs within the $\text{Lin}^- \text{CD34}^+ \text{CD38}^-$ fraction (17). To test whether Rho efflux marked HSCs in conjunction with Thy1 , we transplanted limiting numbers of Thy1^+ cells sorted based on high ($\text{Thy1}^+ \text{Rho}^{\text{lo}}$; Fig. 1, P6) and low ($\text{Thy1}^+ \text{Rho}^{\text{hi}}$; Fig. 1, P7) Rho efflux. Recipients of $\text{Thy1}^+ \text{Rho}^{\text{lo}}$ cells exhibited 40-fold higher chimerism in the

injected femur (fig. S11) and displayed twofold enrichment for HSCs as compared to Thy1^+ alone (table S1).

We next questioned whether the addition of Rho to $\text{Thy1}^+ \text{CD49f}^+$ would permit robust engraftment of single human HSCs. We flow-sorted single $\text{Thy1}^+ \text{Rho}^{\text{lo}} \text{CD49f}^+$ cells and transplanted them into NSG recipients (Fig. 4A). In our first experiment, 5 of 18 recipients (28%, Fig. 4B) transplanted with single cells displayed multilineage chimerism 20 weeks after transplant (Fig. 4C and fig. S12). Serial transfer was successful in two of four secondary recipients despite the fact that only 20% of total marrow was used for transplantation (fig. S13), indicating that individual $\text{Thy1}^+ \text{Rho}^{\text{lo}} \text{CD49f}^+$ cells extensively self-renew. In a second experiment, we observed a lower frequency (14%) of single-cell transfer, perhaps reflecting the genetic heterogeneity of CB donors (Fig. 4B). Human cell engraftment at marrow sites distant from the injected femur indicated that single $\text{Thy1}^+ \text{Rho}^{\text{lo}} \text{CD49f}^+$ cells could give rise to systemic grafts (Fig. 4, D to E), fulfilling a key criterion of HSCs. Based on historical data showing xenotransplantation inefficiency (18), we are probably underestimating HSC frequency. Engraftment of single $\text{Lin}^- \text{CD34}^+ \text{CD38}^- \text{CD45RA}^+ \text{Thy1}^+ \text{Rho}^{\text{lo}} \text{CD49f}^+$ cells provides evidence that human HSCs express CD49f.

In this study, we purified human HSCs at single-cell resolution, separated HSCs from MPPs, and identified $\text{CD34}^+ \text{Thy1}^-$ HSCs. The ability to investigate two highly enriched and related multipotent cell populations that differ in their capacity for self-renewal opens the way for studies to elu-

cidate developmental programs specific to human HSCs. Because the cell number required for chromatin immunoprecipitation coupled with high-throughput sequencing (ChIP-seq) and DNA methylation profiling is constantly decreasing (19–21), it will be critical to subject HSCs and MPPs to these technologies. Such analyses will aid in identifying gene regulatory networks that govern human HSC function and in turn facilitate manipulating and expanding human HSCs ex vivo to overcome barriers to successful transplantation.

References and Notes

1. M. Sauvageau, G. Sauvageau, *Cell Stem Cell* **7**, 299 (2010).
2. H. Mayani, W. Dragowska, P. M. Lansdorp, *Blood* **82**, 2664 (1993).
3. C. M. Baum, I. L. Weissman, A. S. Tsukamoto, A. M. Buckle, B. Peault, *Proc. Natl. Acad. Sci. U.S.A.* **89**, 2804 (1992).
4. W. Craig, R. Kay, R. L. Cutler, P. M. Lansdorp, *J. Exp. Med.* **177**, 1331 (1993).
5. R. Majeti, C. Y. Park, I. L. Weissman, *Cell Stem Cell* **1**, 635 (2007).
6. Q. L. Hao, A. J. Shah, F. T. Thiemann, E. M. Smogorzewska, G. M. Crooks, *Blood* **86**, 3745 (1995).
7. M. Bhatia, J. C. Wang, U. Kapp, D. Bonnet, J. E. Dick, *Proc. Natl. Acad. Sci. U.S.A.* **94**, 5320 (1997).
8. L. D. Shultz et al., *J. Immunol.* **174**, 6477 (2005).
9. J. L. McKenzie, O. I. Gan, M. Doedens, J. E. Dick, *Blood* **106**, 1259 (2005).
10. F. Notta, S. Doulatov, J. E. Dick, *Blood* **115**, 3704 (2010).
11. H. Ueno et al., *Nat. Immunol.* **4**, 457 (2003).
12. J. Stingl et al., *Nature* **439**, 993 (2006).
13. P. Benveniste et al., *Cell Stem Cell* **6**, 48 (2010).
14. M. J. Kiel et al., *Cell* **121**, 1109 (2005).
15. S. Doulatov et al., *Nat. Immunol.* **11**, 585 (2010).
16. M. Osawa, K. Hanada, H. Hamada, H. Nakauchi, *Science* **273**, 242 (1996).
17. J. L. McKenzie, K. Takenaka, O. I. Gan, M. Doedens, J. E. Dick, *Blood* **109**, 543 (2007).
18. L. D. Shultz, F. Ishikawa, D. L. Greiner, *Nat. Rev. Immunol.* **7**, 118 (2007).
19. M. Adli, J. Zhu, B. E. Bernstein, *Nat. Methods* **7**, 615 (2010).
20. A. Goren et al., *Nat. Methods* **7**, 47 (2010).
21. H. Ji et al., *Nature* **467**, 338 (2010).

Acknowledgments: We thank K. Moore and the obstetrics unit of Trillium Hospital (Mississauga, Ontario) for providing CB, the Dick Lab and M. Cooper for critical manuscript review, C. Nostro from the Keller lab for assistance with immunofluorescence, and P. A. Penttilä and the University Health Network/Sickkids flow cytometry facility. This work was supported by Canadian Institutes for Health Research (CIHR) studentships (F.N. and S.D.) and Swiss National Science Foundation and Roche fellowships (E.L.). Grants were received from the CIHR, Canadian Cancer Society, Terry Fox Foundation, Genome Canada through the Ontario Genomics Institute, Ontario Institute for Cancer Research with funds from the province of Ontario, and a Canada Research Chair. This research was funded in part by the Ontario Ministry of Health and Long Term Care (OMOHLTC). The views expressed do not necessarily reflect those of the OMOHLTC. Microarray data are available online at the Gene Expression Omnibus Web page (accession code GSE29105). F.N., S.D., and J.E.D. designed the study; F.N., S.D., and A.P. performed experiments; E.L., S.D., and I.J. analyzed gene expression data; F.N. prepared the manuscript; S.D. and J.E.D. edited the manuscript; and J.E.D. supervised the study.

Supporting Online Material

www.sciencemag.org/cgi/content/full/333/6039/218/DC1
 Materials and Methods
 Figs. S1 to S14
 Tables S1 to S5
 References

3 December 2010; accepted 2 June 2011
 10.1126/science.1201219

Fig. 4. Engraftment of single human HSCs. **(A)** Experimental design used to sort and transplant single P10 ($\text{Thy1}^+ \text{Rho}^{\text{lo}} \text{CD49f}^+$) cells into NSG mice. (1) Single-cell fluorescence-activated cell sorting deposition and microscopic visualization to verify the presence of a single cell. (2) Uptake into syringe. (3) Verification of cell aspiration. (4) Transplant into NSG mice. **(B)** Cloning efficiency, **(C)** B-lymphoid (CD19^+) and myeloid (CD33^+) lineage distribution, and **(D)** mean levels of human chimerism in the injected femur and non-injected bones of single human $\text{Thy1}^+ \text{Rho}^{\text{lo}} \text{CD49f}^+$ HSCs from two independent CB samples engrafting NSG mice. **(E)** Flow cytometric analysis of three representative mice engrafted with single $\text{Thy1}^+ \text{Rho}^{\text{lo}} \text{CD49f}^+$ cells. Auto, auto-fluorescence.

